World Academy of Science, Engineering and Technology
International Journal of Mechanical and Mechatronics Engineering
Vol:8, No:8, 2014

Impact Deformation and Fracture Behaviour of Cobalt-Based Haynes 188 Superalloy

Woei-Shyan Lee, Hao-Chien Kao

***Abstract*—**The impact deformation and fracture behaviour of cobalt-based Haynes 188 superalloy are investigated by means of a split Hopkinson pressure bar. Impact tests are performed at strain rates ranging from 1×103 s-1 to 5×103 s-1 and temperatures between 25°C and 800°C. The experimental results indicate that the flow response and fracture characteristics of cobalt-based Haynes 188 superalloy are significantly dependent on the strain rate and temperature. The flow stress, work hardening rate and strain rate sensitivity all increase with increasing strain rate or decreasing temperature. It is shown that the impact response of the Haynes 188 specimens is adequately described by the Zerilli-Armstrong fcc model. The fracture analysis results indicate that the Haynes 188 specimens fail predominantly as the result of intensive localised shearing. Furthermore, it is shown that the flow localisation effect leads to the formation of adiabatic shear bands. The fracture surfaces of the deformed Haynes 188 specimens are characterised by dimple- and / or cleavage-like structure with knobby features. The knobby features are thought to be the result of a rise in the local temperature to a value greater than the melting point.

***Keywords*—**Haynes 188 alloy, impact, strain rate and temperature effect, adiabatic shearing.

I. Introduction

HAYNES 188 superalloy has many favourable properties, including good strength at high temperatures; excellent ductility, fabricability and weldability. It is currently used for fabricating the combustor liners in aircraft turbine engines and the liquid oxygen posts in the main injector of the space shuttle engines [1], [2]. In such applications, the components are subjected to extremely high temperatures and strain rates during their fabrication and subsequent service lives. The literature contains many investigations into the mechanical properties of Haynes 188 alloy under high temperatures [3], [4]. However, the high temperature deformation behaviour and deformation-induced microstructure of Haynes 188 under high strain rate loads have attracted little attention thus far. Previous studies have shown that the deformation behaviour of most metals and alloys is significantly dependent on the strain rate and temperature. Specifically, the flow stress increases rapidly with increasing strain rate or decreasing temperature [5], [6]. Under high strain rate adiabatic loading conditions, the plastic deformation becomes unstable and adiabatic shear bands are formed due to a localisation of the plastic flow. The adiabatic shear bands act as preferential sites of crack initiation and are therefore a major cause of dynamic failure. As a result, the initiation and growth of adiabatic shear bands have been investigated for a wide range of metals and alloys [7]-[9].The present study investigates the mechanical properties and deformation substructure of Haynes 188 superalloy at temperatures ranging from 25 ~ 800ºC and strain rates ranging from $1x10^3 \sim 5x10^3$ s^{-1} using a split-Hopkinson pressure bar (SHPB) system. The correlation between the microstructural evolution of the impacted specimens and the mechanical response is systematically examined and discussed.

W.S. Lee is with the National Cheng Kung University, Department of Mechanical Engineering, Tainan, 70101Taiwan (phone: 886-6-2757575 ext. 62174; fax: 886-6-2352973; e-mail: wslee@mail.ncku.edu.tw).

H.C. Kao is with the National Cheng Kung University, Department of Mechanical Engineering, Tainan, 70101Taiwan (phone: 886-6-2757575 ext. 62159-34; fax: 886-6-2352973; e-mail: n16011655@mail.ncku.edu.tw).

II. Experimental Procedure

The Haynes 188 alloy used in the present tests was supplied by Aero Win Technology Corp. (Taiwan, R.O.C) in the form of hot-rolled, solution-annealed bar with a diameter of 15 mm. (Note that solution annealing was performed at 1175ºC for 1 hour followed by water quenching.). The alloy had a chemical composition (wt. pct) of 22.43 Ni, 21.84 Cr, 13.95 W, 1.24 Fe, 0.01 C, 0.75 Mn, 0.40 Si, 0.012 P, 0.002 S, 0.034 La, 0.002 B, and a balance of Co. Cylindrical specimens with a length of 7±0.1 mm and a diameter of 7.1 mm were machined from the as-received bar and finished to a final diameter of 7±0.1 mm via a centre-grinding process. The end faces of the specimens tested at room temperature (25ºC) were lubricated with commercial molybdenum disulfide (Molykote), while those tested at elevated temperatures were lubricated using a glass paste consisting of a powder of 80% P_bO and 20% B_2O_3 mixed with alcohol.

The specimens were deformed at temperatures of 25ºC, 400ºC and 800ºC and strain rates of $1x10^3$ s^{-1}, $3x10^3$ s^{-1} and $5x10^3$ s^{-1} using a SHPB system. This device utilizes measurements of elastic waves in hardened steel pressure bars to determine the relative motion of the two faces of the test specimen and the associated stress. A full description of a split-Hopkinson pressure bar and its utilization for obtaining dynamic properties data is included in reference [10]. In addition, the modification of the calculations for the strain, strain rate and stress at elevated temperatures is shown in [11]. Finally, the surfaces of the fractured specimens were observed using a FEI Quanta 400 F scanning electron microscope with an operating voltage of 30 kV.

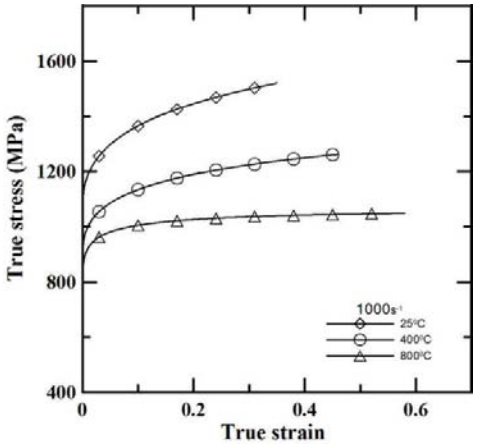

Fig. 1 (a) Stress-strain curves of Haynes 188 alloy deformed at temperatures of 25 ~ 800ºC and strain rates of$1x10^3$ s^{-1}

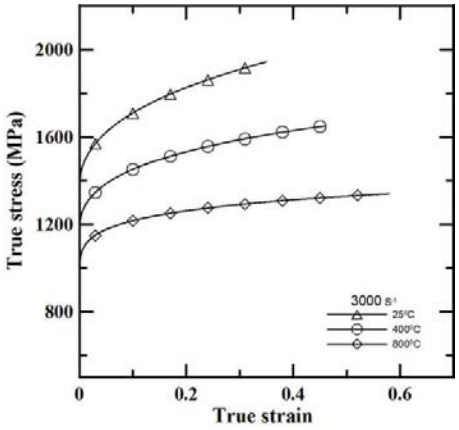

Fig. 1 (b) Stress-strain curves of Haynes 188 alloy deformed at temperatures of 25 ~ 800ºC and strain rates of$3x10^3$ s^{-1}

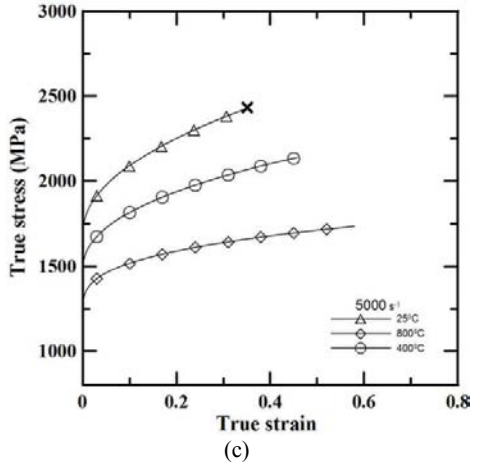

(c)

Fig. 1 (c) Stress-strain curves of Haynes 188 alloy deformed at temperatures of 25 ~ 800ºC and strain rates of $5x10^3$ s^{-1}

III. Results and Discussions

Figs. 1 (a)~(c) show the stress-strain curves of the impacted Haynes 188 specimens. It can be seen that the flow response of all the specimens is significantly dependent on both the strain rate and the temperature. For a constant strain rate, the flow stress decreases with increasing temperature, but the true strain increases. Moreover, for a constant temperature, the maximum strain increases with increasing strain rate. Overall, it is seen that the strain rate has a greater effect on the flow stress than the temperature. It is observed that the flow stress increases more rapidly with increasing true strain at lower temperatures and higher strain rates. In other words, the work hardening rate during plastic deformation increases as the temperature is reduced or the strain rate increased. In addition, it is seen that specimen fracture occurs only at the highest strain rate of 5×10^3 s^{-1} and the lowest temperature of 25ºC. Thus, it is inferred that Haynes 188 alloy has good deformability and strengthening properties at high temperatures; even when deformed to large strains.

The stress-strain curves presented in Fig. 1 show that the specimens deformed at different strain rates and temperatures have a different work hardening response. In general, the stress-strain response of engineering metals and alloys can be described by the power law $\sigma = A + B\varepsilon^n$, where A is the yield strength, B is the material constant and n is the work hardening coefficient. Table I presents the results obtained for A, B and n for the present Haynes 188 specimens under the considered loading conditions. It is seen that for a given temperature, the yield strength, material constant and work hardening coefficient all increase with increasing strain rate. Thus, it is inferred that the dislocation density and multiplication rate increase at higher strain rates and give rise to an enhanced flow resistance. However, for a given strain rate, the yield strength, material constant and work hardening coefficient all decrease with increasing temperature. The reduction in the yield strength and work hardening coefficient with increasing temperature is due to a reduction in the density and rate of multiplication of the dislocations at higher temperatures, which results in a lower resistance to plastic flow and a more ductile behaviour.

TABLE I
Mechanical Properties of Haynes 188 Alloy Deformed at Temperature of 25 ~ 800ºC and Strain Rates of $1x10^3 \sim 5x10^3$ s^{-1}

T (°C)	Strain rate (s^{-1})	Yield stress *A* (MPa)	Material constant *B* (MPa)	Work hardening coefficient *n*
25	1000	1038.06	707.32	0.34
	3000	1349.65	912.04	0.40
	5000	1692.71	1228.19	0.49
400	1000	832.51	534.61	0.25
	3000	1141.56	672.12	0.34
	5000	1472.36	938.76	0.44
800	1000	538.32	550.65	0.07
	3000	899.62	492.95	0.20
	5000	1227.94	601.75	0.32

Fig. 2 (a) shows the variation of the flow stress with the strain rate as a function of the deformation temperature and strain. It is seen that for all three temperatures, the flow stress increases dramatically with both an increasing strain rate and an increasing strain. The greater flow stress at higher strain rates suggests that the dynamic deformation behaviour of Haynes 188 alloy is governed by the effects of thermal activation in

enabling dislocations in the deformed microstructure to overcome short-range barriers to motion [12]. Furthermore, the dynamic behaviour of the present Haynes 188 alloy is significantly dependent on the deformation temperature. Fig. 2 (b) shows the variation of the flow stress with the deformation temperature as a function of the strain and strain rate. It can be seen that the flow stress decreases linearly with increasing temperature at all values of the strain and strain rate. The linear dependence of the flow stress on the temperature is consistent with the findings of Guo et al. for Nitronic-50 [13] and can be adequately described using the constitutive equation proposed by Litonski [14].

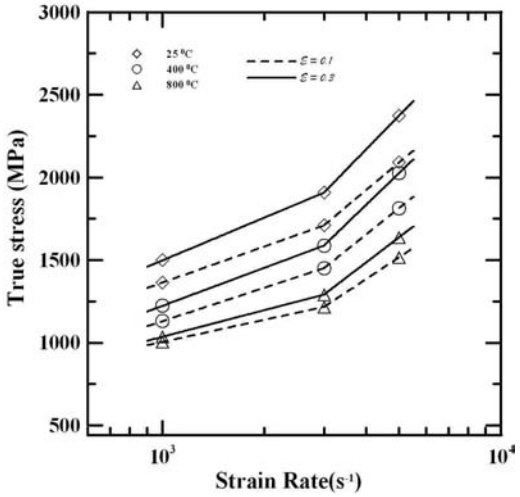

Fig. 2 (a) Variation of true stress with logarithmic strain rate as function of temperature and true strain

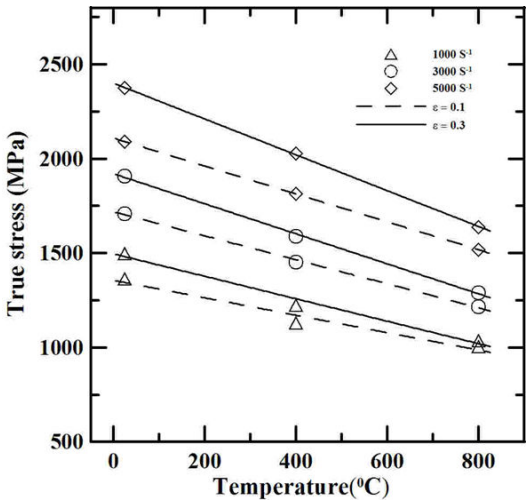

Fig. 2 (b) Variation of flow stress with deformation temperature as function of strain and strain rate

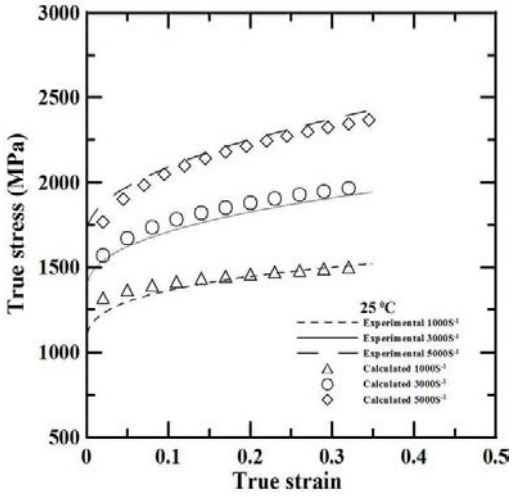

Fig. 3 (a) Comparison of predicted and experimental stress-strain curves for Haynes 188 alloy deformed at temperatures of 25ºC

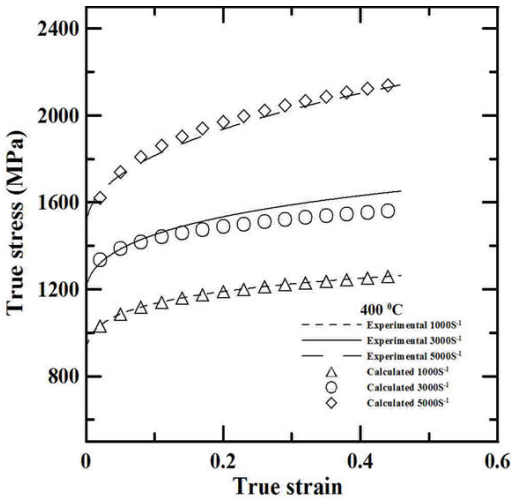

Fig. 3 (b) Comparison of predicted and experimental stress-strain curves for Haynes 188 alloy deformed at temperatures of 400ºC

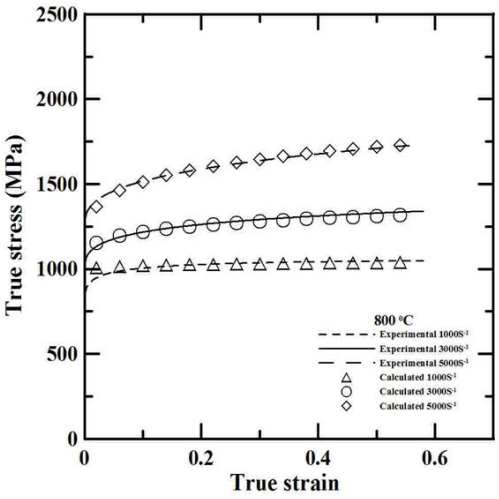

Fig. 3 (c) Comparison of predicted and experimental stress-strain curves for Haynes 188 alloy deformed at temperatures of 800ºC

In examining the reliability of structural designs using a finite element analysis (FEA) approach, it is beneficial to describe the material behavior using some form of constitutive relation amenable to implementation in computer code. The literature contains many constitutive models for describing the mechanical behaviour of engineering metals and alloys [15]-[17]. In this study, the high strain rate, high temperature mechanical response of Haynes 188 alloy is described using the Zerilli-Armstrong fcc model, i.e., [15]

$$\sigma = C_o + C_2 \varepsilon^{1/2} [\exp(-C_3 T + C_4 T \ln \dot{\varepsilon})] \quad (1)$$

where C_0, C_2, C_3 and C_4 are constants; σ is the stress; ε is the equivalent plastic strain; $\dot{\varepsilon}$ is the strain rate; and T is the deformation temperature. By applying a regression analysis technique to the true stress-strain data presented in Figs. 1 (a)-(c), the constants in (1) were found to be as follows: C_0 = 1011.2 MPa; C_2 =2244.67 MPa; C_3 = 1.7×10^{-2}(K^{-1}) and C_4 = 1.9×10^{-3}(K^{-1}). Figs. 3 (a)-(c) compare the experimental stress-strain curves given in Fig. 3 with those predicted using (1) for strain rates of $1x10^3 \sim 5x10^3$ s^{-1} and temperatures of 25ºC, 400ºC and 800ºC, respectively. It is seen that the Zerilli-Armstrong model provides an adequate description of the dynamic response of Haynes 188 alloy under the high strain rate and high temperature loading conditions considered in the present study.

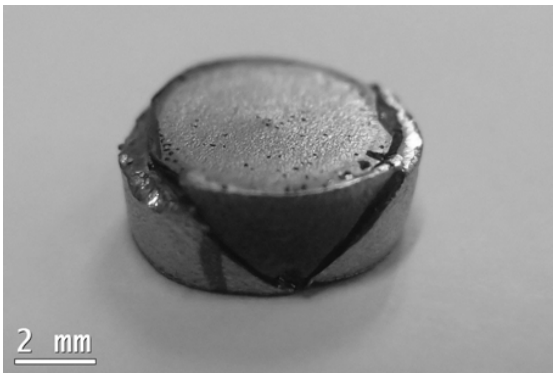

Fig. 4 (a) Photograph showing fracture features of Haynes 188 specimen deformed at 25ºC and $5x10^3$ s^{-1}

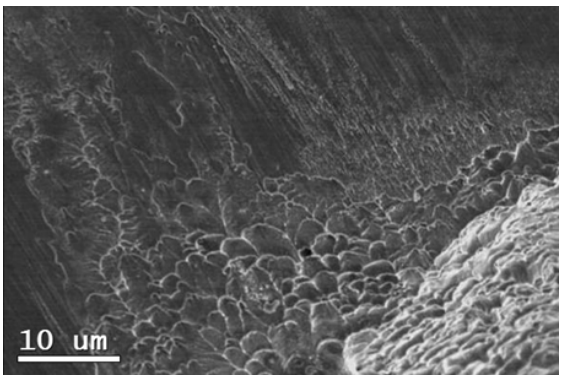

Fig. 4 (b) SEM micrograph of fracture surface in Fig. 4 (a)

Of all the impacted specimens, only the specimen tested at a temperature of 25ºC and a strain rate of $5x10^3$ s^{-1} failed. As shown in Fig. 4 (a), the specimen failed as a result of adiabatic shearing along two planes orientated at angles of 40~50º with respect to the impact direction. Moreover, as shown in Fig. 4 (b), the fracture surface is characterised by both cleavage features (labeled A) and dimple structures (labeled B) as the result of adiabatic shearing. In addition, knobby features (labeled C) are seen near the dimple structure zone. The presence of these knobby features suggests that the local temperature exceeded the melting point of Haynes 188 alloy (i.e., 1330°C) during the impact event.

IV. Conclusions

The experimental results indicate that the flow stress of Haynes 188 alloy is strongly dependent on the temperature and strain rate. Moreover, the strain rate sensitivity reduces, but the temperature sensitivity increases, as the temperature is increased from 400ºC to 800ºC. The Zerilli-Armstrong fcc model provides an adequate description of the flow stress-strain response of Haynes 188 alloy under the considered loading conditions. Specimen fracture occurs only at the lowest temperature of 25ºC and the highest strain rate of $5x10^3$ s^{-1}. In other words, Haynes 188 alloy has good fracture resistance and deformability at high temperatures and strain rates. The SEM observations suggest that specimen failure occurs as the result of adiabatic shearing.

Acknowledgment

The authors gratefully acknowledge the financial support provided to this study by the National Science Council (NSC) of Taiwan under Contract No. NSC101-2221-E-006-144.

References

[1] Haynes alloy 188, Report-Haynes International, Inc., Kokomo, TN, 1991.
[2] G. R. Halford, J. F. Saltsman, S. Kalluri, " High Temperature Fatigue Behaviour of Haynes 188,"edited by R. J. Richmond and S. T. Wu., Proc. Advanced Earth-to-Orbit Propulsion Technology Conf., MSFC, Huntsville, AL, NASA CP-3012, NASA, Washington, DC, 18-988, May 10-13, 1988, pp. 497-507.
[3] S. Y. Lee, Y. L. Lu, P. K. Liaw, H. Choo, S. A. Thompson, J. W. Blust, P. F. Browning, A. K. Bhattacharaya, J. M. Aurrecoechea and D. L. Klarstrom, "High-temperature tensile-hold crack-growth behaviorof HASTELLOY® X alloy compared to HAYNES® 188and HAYNES® 230® alloys," *Mech. Time-Depend. Mate.* 12, 31-44 (2008).
[4] P. J. Bonacuse and S. Kalluri,"Elevated Temperature Axial and Torsional Fatigue Behavior of Haynes 188,"*J. Eng. Mater. Tech.* 117, 191-199 (1995).
[5] S. Nemat-Nasser, Y. F. Li, J.B. Isaacs,"Experimental/ computational evaluation of flow stress at high strain rates with application to adiabatic shear banding," *Mech. Mater.* 17,111-134(1994).
[6] M.A. Meyers, Y.J. Chen, F.D.S.Marguis and D.S. Kim," High-strain, high strain-rate behavior of tantalum" *Metall. Mater. Trans. A*26, 2493-2501 (1995).
[7] A. G. Odeshi and M. N. Bassim,"High strain-rate fracture and failure of a high strength low alloy steel in compression," *Mater. Sci. Eng. A* 525, 96-101(2009).
[8] WR. C. Batra and D. Liu,"Adiabaticshear banding in plane strain problems," *ASME J. Appl. Mech.* 56, 527-534(1989).
[9] L. E. Murr, A. C. Ramirez, S. M. Gaytan,M. I. Lopez,E. Y. Martinez,D. H. Hernandez and E. Martinez, "Microstructure evolution associated with adiabatic shear bands and shear band failure in ballistic plug formation in Ti–6Al–4V targets," *Mater. Sci. Eng. A* 516, 205-216(2009).

[10] U.S. Lindholm," Some experiments with the split hopkinson pressure bar∗," *J. Mech. Phys. Sol.* 12, 317-335 (1964).
[11] W. S. Lee and C. F. Lin,"Plastic deformation and fracture behaviour of Ti–6Al–4V alloy loaded with high strain rate under various temperatures," *Mater. Sci. Eng. A*. 241,48-59(1998).
[12] P. S. Follansbee and U. F. Kocks," A constitutive description of the deformation of copper based on the use of the mechanical threshold stress as an internal state variable,"*Acta Metall.* 36, 81-93(1988).
[13] W. G. Guo and S. Nemat-Nasser,"Flow stress of Nitronic-50 stainless steel over a wide range of strain rates and temperatures."*Mech. Mater.* 38, 1090-1103 (2006).
[14] J. Litonski," Plastic Flow of a Tube Under Adiabatic Torsion," *Bull. Acad. Pol. Sci. Ser. Sci. Technol.* 25, 7–14(1977).
[15] F. J. Zerilli and R. W. Armstrong," Dislocation-mechanics based constitutive relations for material dynamics calculations,"*J. Appl. Phys.*61(5), 1816-1825 (1987).
[16] S. R. Bodner, and Y. Partom," Constitutive equations for elastic strain-hardening meterials,"*J. Appl. Mech.* 385-389(1975).
[17] A. S. Khan, Y. S. Suh and R. Kazmi," Quasi-static and dynamic loading responses and constitutive modeling of titanium alloys,"*Int. J. Plasticity* 20, 2233-2248(2004).